ACS APPLIED MATERIALS & INTERFACES

Research Article

www.acsami.org

# High-Energy Redox-Flow Batteries with Hybrid Metal Foam Electrodes

Min-Sik Park,[†] Nam-Jin Lee,[†] Seung-Wook Lee,[†] Ki Jae Kim,*[,†] Duk-Jin Oh,[§] and Young-Jun Kim*[,†]

[†]Advanced Batteries Research Center, Korea Electronics Technology Institute, 68 Yatap-dong, Bundang-gu, Seongnam 463-816, Republic of Korea

[§]Battery Group, Samsung Advanced Institute of Technology, Samsung Electronics, Yongin 446-712, Republic of Korea

Supporting Information

**ABSTRACT:** A nonaqueous redox-flow battery employing $[Co(bpy)_3]^{+/2+}$ and $[Fe(bpy)_3]^{2+/3+}$ redox couples is proposed for use in large-scale energy-storage applications. We successfully demonstrate a redox-flow battery with a practical operating voltage of over 2.1 V and an energy efficiency of 85% through a rational cell design. By utilizing carbon-coated Ni-FeCrAl and Cu metal foam electrodes, the electrochemical reactivity and stability of the nonaqueous redox-flow battery can be considerably enhanced. Our approach intoduces a more efficient conversion of chemical energy into electrical energy and enhances long-term cell durability. The cell exhibits an outstanding cyclic performance of more than 300 cycles without any significant loss of energy efficiency. Considering the increasing demands for efficient energy storage, our achievement provides insight into a possible development pathway for nonaqueous redox-flow batteries with high energy densities.

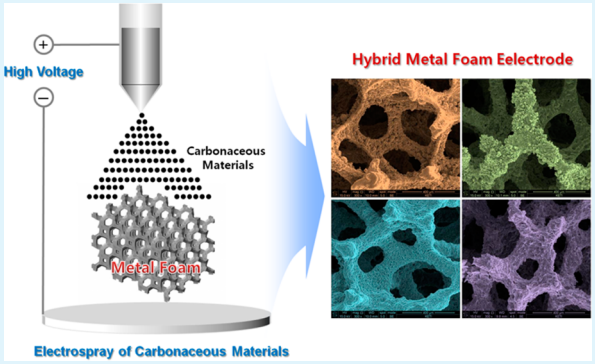


**KEYWORDS:** *redox-flow battery, metal foam, nonaqueous electrolyte, electrode*

## INTRODUCTION

Increasing oil prices and climate change driven by greenhouse gas emission have stimulated unprecedented levels of interest in renewable energy production, as well as the development of environmentally sustainable and inexpensive energy-storage systems with high specific energies. Considering the rapid growth of the market for large-scale energy-storage systems, improving the capacity and efficiency of these systems is regarded as a key technological challenge.[1−3] Among the various energy-storage systems currently under development, the redox-flow battery (RFB) is an attractive candidate for use in large-scale applications.

RFBs offer remarkable advantages, such as reliability, durability, and high power, over other competitive systems.[4−6] In a RFB, electrical energy can be stored in a given mass through chemical redox reactions between different electroactive species dissolved in electrolytes, referred to as catholytes and anolytes. Both electrolytes are separated by an ion-exchange membrane and circulated through the cell composed of porous electrodes and bipolar plates. Chemical redox reactions occur mainly on the surfaces of the electrodes and generate electrical charges that are easily conducted through the electrodes. In this type of system, proper electrolyte and electrode design are essential for achieving optimal cell performance.[7−12]

Recently, remarkable progress has been reported in all-vanadium RFBs (VRFBs) based on aqueous mixed sulfate and chloride electrolytes in which carbon felt was employed as the electrode. VRFBs are composed of $V^{2+}/V^{3+}$ and $V^{4+}/V^{5+}$ redox couples with an operating voltage of 1.25 V that enables them to deliver high energy efficiencies of ∼85% over a wide operational temperature window.[13] These recent advances are impressive and are considered a step toward RFB commercialization. However, in principle, the cell potential of a RFB incorporating aqueous electrolytes is limited by water electrolysis because water is only electrochemically stable within a narrow potential window, theoretically below 1.6 V.[14−17] Given this issue, there is an increasing level of interest in nonaqueous electrolytes with higher redox potentials and wider potential windows, both of which are mainly responsible for improved energy and power densities in RFBs. Up to this point, various nonaqueous electrolytes with redox couples, such as Zn/Ce,[18,19] $Ru(bpy)_3$,[20] and $M(acac)_3$ (M = V, Cr, Mn),[21] and various metal complexes[22,23] have been proposed and investigated for potential use. However, further analyses of the feasibility of such nonaqueous RFBs are still required.

Another important advantage of nonaqueous electrolytes is that metal electrodes can be used unmodified without severe chemical corrosion. Metal electrodes have many advantages, including high electrical conductivity, good mechanical properties, and reasonable price compared to conventional carbon-based electrodes. Despite these promising features, only a few

Received: April 29, 2014
Accepted: June 6, 2014
Published: June 6, 2014

  

studies have focused on the use of noble-metal electrodes in nonaqueous RFBs.[24] These noble metals are expensive, although they possess excellent reactivity for redox reactions. It would be benefical, therefore, to find suitable metal electrodes for use in nonaqueous RFBs and diagnose their advantages.

Herein, we present an exact diagnosis for the utilization of nonaqueous electrolytes and metal foam electrodes from an electrochemical point of view. We propose the use of nonaqueous electrolytes containing $[Co(bpy)_3]^{+/2+}$ and $[Fe(bpy)_3]^{2+/3+}$ redox couples as the anolyte and catholyte, respectively, and evaluate their electrochemical performance. Porous metal foams were employed as the electrodes in our proposed system. For practical reasons, various carbon-based materials were coated on the surface of the metal foam electrodes by electrospray deposition to provide large surface areas. This is perhaps the most challenging aspect of this work. On the basis of various structural and electrochemical analyses, a correlation between the electrochemical activities of the carbon-coated metal foam electrodes and their morphological characteristics is demonstrated. Our approach is quite promising for improving the electrochemical reactivity and stability of metal foam electrodes in RFBs.

## EXPERIMENTAL SECTION

**Preparation of Nonaqueous Electrolytes.** The anolyte was prepared by dissolving 0.2 M tris(2,2′-bipyridine)cobalt tetrafluoroborate $[Co(bpy)_3(BF_4)_2$; HANCHEM] and 0.5 M tetraethylammonium tetrafluoroborate ($TEABF_4$; Aldrich) as the supporting electrolyte in a propylene carbonate solution (PC; PANAX ETEC). To prepare the catholyte, 0.2 M tris(2,2′-bipyridine)iron tetrafluoroborate $[Fe(bpy)_3(BF_4)_2]$ was dissolved in PC with the same supporting electrolyte. To remove dissolved oxygen, both electrolytes were purged for at least 10 min with dry $N_2$.

**Fabrication of Carbon-Coated Metal Foam Electrodes.** Ni-FeCrAl (a Ni-based multicomponent alloy) and Cu foams (Alantum Corp.) were selected as the positive and negative electrodes, respectively. The metal foams were etched with a 1 M HCl solution at room temperature to clean their surfaces before use. Slurries containing various carbon materials (Super-P, VGCF, and graphene) and a poly(vinylidene fluoride) binder in a weight ratio of 7:3 in an *N*-methylpyrrolidone solution were prepared and deposited on the surfaces of the metal foams using an electrospray technique (Figure S1 in the Supporting Information, SI). The amounts of deposited carbon materials were controlled using the amount electrosprayed (8 mL), the rate of deposition (4 mL $h^{-1}$), and the coated area (33.0 $cm^2$) as parameters. After carbon deposition, the metal foams were dried in a vacuum oven at 120 °C for 12 h.

**Structural Characterization.** The morphologies of the Ni-FeCrAl and Cu foams were examined using field-emission scanning electronic microscopy (FESEM; JEOL JSM-7000F). The microstructures of the metal foams were investigated using a high-resolution microcomputed tomography (micro-CT) scanner (SkyScan1172, Bruker) and an associated X-ray source (voltage = 100 kV and current = 100 $\mu$A). The rotation increment and exposure time were fixed at 0.5° and 140 ms, respectively. The specific surface area and total porosity were estimated from the results. The electrical conductivities of carbon layers deposited on the metal substrates were measured using the four-point probe method (LORESTA-GP). The surface area and pore volume of the carbon materials were measured using the Brunauer–Emmett–Teller (BET) and Barrett–Joyner–Halenda methods, respectively, using a porosimetry analyzer (Tristar II 3020, Micromeritics). The ion crossover in the proposed system was evaluated by inductively coupled plasma mass spectroscopy (ICP-MS; Bruker aurora M90).

**Cell Configurations and Electrochemical Characterizations.** A test cell was constructed from the Ni-FeCrAl and Cu foams used as electrodes (14.7 cm × 8.8 cm), an ion-exchange membrane, and bipolar plates. The ion-exchange membrane (Fumapem, F-14100) and bipolar plates (Morgan Korea Co. Ltd.) were 15.7 cm × 10.8 cm in size. The degassed electrolytes were stored in separate reservoirs connected with the cell. The main components were assembled in an order following the flow path (Figure S2 in the SI). The cell frames were insulated with Teflon films to prevent undesirable current loss during cycling. To evaluate their electrochemical properties, the cells were galvanostatically charged and discharged over a voltage range of 1.7–2.1 V at a current density of 1.2 mA $cm^{-2}$. Each electrolyte passed through an inlet with an inner diameter of 4.8 mm and circulated inside the cell. The flow rate of the auxiliary pumps connected with the cell was fixed at 1.37 mL $s^{-1}$. Cyclic voltammetry (CV) measurements were carried out using a potentiostat/galvanostat (EC-Lab, BioLogic) in a three-electrode glass cell consisting of metal foam working electrodes, a platinum mesh counter electrode, and an $Ag/Ag^+$ reference electrode at various scan rates from 5 to 100 mV $s^{-1}$.

## RESULTS AND DISCUSSION

**Electrochemical Properties of $[Fe(bpy)_3]^{2+/3+}$ and $[Co(bpy)_3]^{+/2+}$ Redox Couples.** In pursuit of high-energy RFBs, we investigated the electrochemical properties of nonaqueous electrolytes with $[Fe(bpy)_3]^{2+/3+}$ (catholyte) and $[Co(bpy)_3]^{+/2+}$ (anolyte) redox couples. The choice of the redox couple was made based on a comparison of the theoretical redox potentials for various metal ions in aqueous solutions. The proposed redox couples were designed as metal complexes composed of selected metal ions and $(bpy)_3$, as shown in Figure 1a,b.

The electrochemical reactivity of both metal complexes involved in the proposed electrolytes has been examined by CV using a glassy carbon electrode under optimized conditions. According to the CV profiles (Figure S3 in the SI), the $Co(bpy)_3$ metal complex clearly exhibited four redox peaks related to the oxidation and reduction of $[Co(bpy)_3]^{+/2+}$ around −1.4 V and the redox reaction of $[Co(bpy)_3]^{2+/3+}$ in a more positive potential region around 0 V. The $Fe(bpy)_3$ metal complex also showed distinctive redox reactions around 0 V for $[Fe(bpy)_3]^{+/2+}$ and 0.7 V for $[Fe(bpy)_3]^{2+/3+}$. Note that the redox couples can be reversibly oxidized and reduced in the given potential window without undesirable side reactions.

On the basis of the electrochemical reactivity of $Fe(bpy)_3$ and $Co(bpy)_3$, we designed overall redox reactions coupled with $[Fe(bpy)_3]^{2+/3+}$ (catholyte) and $[Co(bpy)_3]^{+/2+}$ (anolyte); these exhibited an operating potential of about 2.16 V, as indicated in Figure 1c. The CV profile shows two distinct redox peaks at −1.39 and −1.51 V, corresponding to the oxidation of $[Co(bpy)_3]^+$ and the reduction of $[Co(bpy)_3]^{2+}$, respectively. The oxidation of $[Fe(bpy)_3]^{2+}$ and the reduction of $[Fe(bpy)_3]^{3+}$ are also observed at positive potentials of 0.65 and 0.54 V, respectively. Furthermore, we confirmed that the electrochemical reactivities of both redox couples were quite stable even after 100 cycles (dotted line), as shown in Figure 1c.

**Physical Properties of Hybrid Metal Foam Electrodes.** Carbonaceous materials, such as carbon felt and carbon fiber, have been widely used as electrodes for aqueous RFBs because of their good chemical stability and durability, while the use of metal electrodes is highly limited because of their poor chemical stability and corrosion resistance in aqueous solutions. These problems, however, are unimportant in nonaqueous systems because the metal electrodes possess tremendous advantages such as good electrical conduction and heat transfer, low production costs, and excellent long-term stability. We have

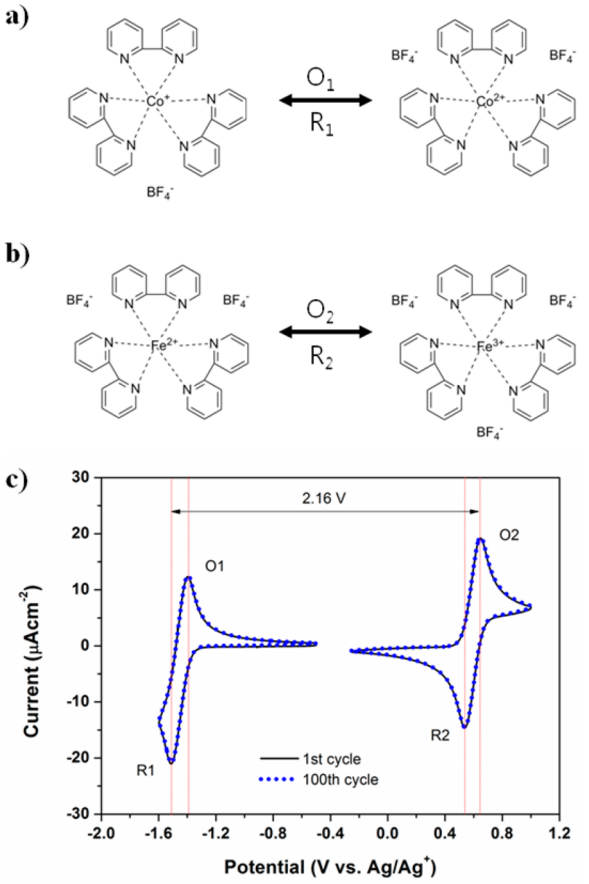


**Figure 1.** Schematic of redox reactions for (a) $[Co(bpy)_3]^{+}$ and $[Co(bpy)_3]^{2+}$ in the anolyte and (b) $[Fe(bpy)_3]^{2+}$ and $[Fe(bpy)_3]^{3+}$ in the catholyte. (c) Cyclic voltammograms for the nonaqueous electrolyte employing $[Co(bpy)_3]^{+/2+}$ and $[Fe(bpy)_3]^{2+/3+}$ redox couples during the 1st and 100th cycles.

explored the use of various metal systems in our previous work,[24] and, among them, Ni-FeCrAl and Cu possess outstanding electrochemical activities in our proposed catholyte and anolyte, respectively. In fact, the electrochemical reactivity of both metals is comparable with that of noble metals such as Pt and Au.[25]

In order to establish flow channels and enhance electric conduction in the electrodes, both metals have been fabricated as a porous metal foam (average pore size of about 800 $\mu$m). The total porosity was maximized (up to 90%) by pore size control methods for efficient energy conversion. FESEM images in Figure 2a show representative views of the Ni-FeCrAl foam at different magnifications. The Ni-FeCrAl foam has a three-dimensional porous structure with a surface area of 0.064 $m^2\ g^{-1}$. Even after maximization of the porosity, however, the surface areas of the Ni-FeCrAl foams are still not large enough to facilitate sufficient redox reactions of the metal complexes in the electrolytes investigated here.

Because the specific interfacial area of the electrodes is directly proportional to the number of reaction sites for the redox reactions, it is important to maximize the specific surface area of the electrodes to improve their electrochemical reactivity. To do this, the metal foam was coated with various carbon-bearing materials (Super-P, VGCF, and graphene) by electrospray deposition from a slurry containing each carbon material and binder (7:3, w/w). The composition of the slurry

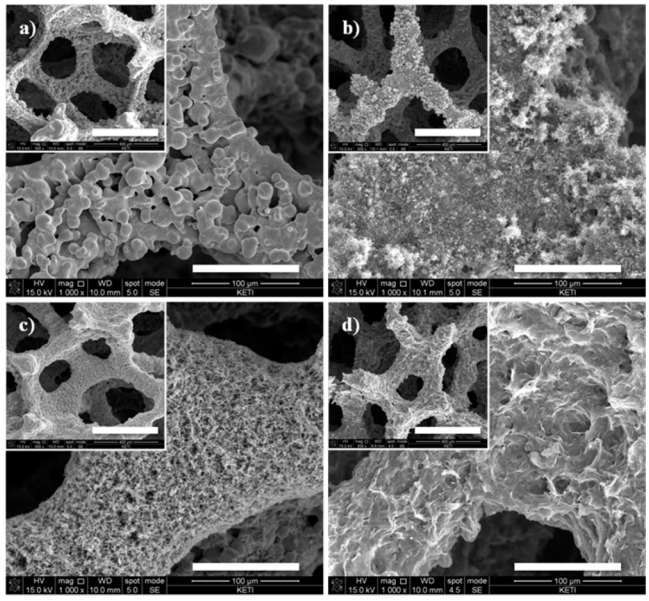


**Figure 2.** FESEM images of (a) bare Ni-FeCrAl foam, (b) Super-P-coated Ni-FeCrAl foam, (c) VGCF-coated Ni-FeCrAl foam, and (d) graphene-coated Ni-FeCrAl foam (scale bar: 100 $\mu$m). Higher-magnification images are inset (scale bar: 400 $\mu$m).

was optimized to ensure the mechanical stability of the carbon layers. This requires the use of a minimal amount of binder because the low electrical conductivity of the binder influences the electrochemical properties of the metal foams. Parts b–d of Figure 2 show the morphologies of the metal foams after electrospray deposition of Super-P, VGCF, and graphene, respectively. According to the FESEM results, the carbon materials were uniformly deposited on the surface of the metal foams and form porous surface layers. This is an effective way to increase the surface area of the metal foams without the undesirable loss of total porosity.

Figure 3 shows the morphologies of the different carbon materials and cross-sectional images of the deposited carbon layers on the metal substrates. The carbon layers exhibit distinctive microstructures according to the nature of the different carbon materials. As can be seen in Figure 3a,b, the Super-P layer exhibits a fine three-dimensional-networked structure of abundant mesopores of less than 100 nm in size. These pores are essential for facilitating the redox reactions and establishing the flow channels. In comparison, the graphene layer provides relatively large macropores (>100 nm in size), as shown in Figure 3c,d. In the VGCF layer, the one-dimensional carbon fibers were randomly distributed, and disordered macropores were also created in the deposited layer, providing sufficient reaction sites and flow channels (Figure 3e,f). The carbon materials deposited by electrospraying maintained their unique structures, leading to the formation of porous carbon layers with different pore structures. It is expected that the deposited porous carbon layers will enhance the electrochemical reactivity of the metal foams by providing more reaction sites for the redox reactions in the RFBs.

For further inspection and characterization, the microstructures of carbon-coated metal foams were imaged using a micro-CT scanner, as shown in Figure 4. The internal structures of the Ni-FeCrAl and Cu foams were reconstructed from the obtained X-ray images. The Ni-FeCrAl and Cu foams have highly porous sructures with a similar pore size of about

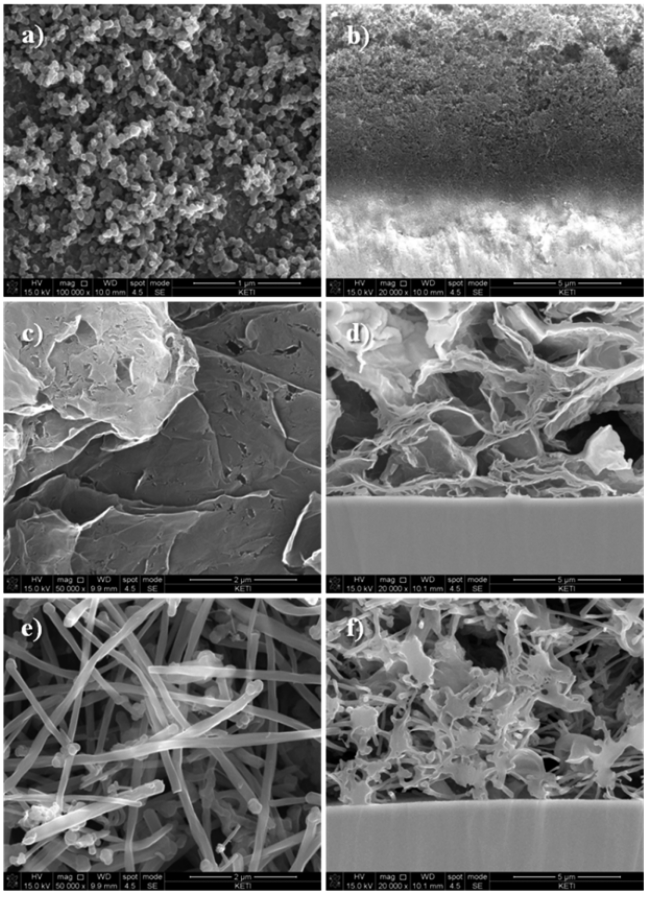


**Figure 3.** FESEM images of the various carbon materials (top view) and cross-sectional images of the deposited carbon layers on the metal substrates prepared by electrospray deposition: (a and b) Super-P; (c and d) graphene; (e and f) VGCF.

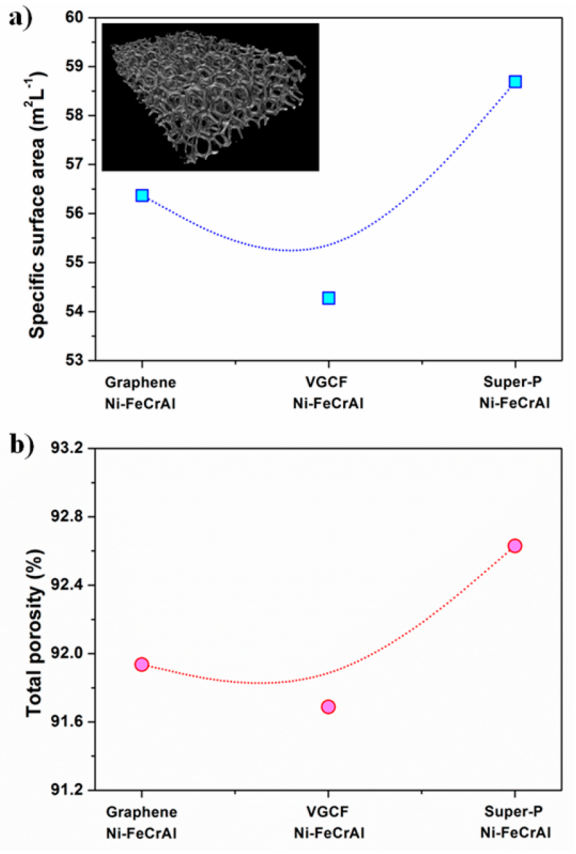


**Figure 4.** Comparisons of (a) the specific surface and (b) total porosity of the Ni-FeCrAl foams after coating with various carbon materials (graphene, VGCF, and Super-P). The values were estimated from the reconstructed image obtained by micro-CT (inset). For more detailed descriptions, the specific surfaces of three-dimensional metal foams with nonuniform pore shapes are represented as the area per unit volume ($m^2$ $L^{-1}$).

800 $\mu$m (inset of Figure 4a), in which the well-developed macropores are interconnected by flow channels. From the reconstructed images (inset of Figure 4a), we can obtain more detailed information on their physical properties such as the specific surface and total porosity, perhaps the most important factors influencing the electrochemical performance of the metal foam electrodes in the RFBs. The specific surface area and total porosity of the Ni-FeCrAl and Cu foams could be notably increased after the deposition of various carbon materials, which would be essential for improving the electrochemical performance of RFBs. All of the carbon-coated metal foams have a similar amount of deposited carbon (~2.7 mg $cm^2$), but their specific surface area and total porosity differ according to the type of deposited carbon material. Upon comparison, the Super-P/Ni-FeCrAl foam shows the largest specific surface area (58.7 $m^2$ $L^{-1}$) because the highest specific surface area of all of the carbon-coated layers is found in the Super-P layer (13.5 $m^2$ $g^{-1}$). The VGCF/Ni-FeCrAl foam shows the lowest specific surface area (54.2 $m^2$ $L^{-1}$). In addition, the Super-P/Ni-FeCrAl foam also exhibited a total porosity of 92.6%, which is higher than those of the metal foams coated with VGFF (91.8%) and graphene (91.7%). The differences in the specific surface area and porosity values mainly originate from the different morphologies of the deposited carbon materials, which is a predominant factor determining the pore structure in the carbon layers formed by electrospray deposition. Even after carbon deposition, the total porosity of the metal foams remained above 90%. We suggest that carbon deposition is appropriate to enlarge the active surface of the metal foams without degrading their pore structures.

With regard to the Cu foam employed as the negative electrode for the oxidation and reduction of $[Co(bpy)_3]^{+/2+}$, these carbon materials have been deposited under the same conditions as those for the Ni-FeCrAl foam. The carbon-coated Cu foams have morphologies and microstructures similar to those of the Ni-FeCrAl foams (Figure S4 in the SI). As expected, similar amounts of the carbon materials were deposited on the surface of Cu foams, which also exhibited different specific surfaces and total porosities according to the type of deposited carbon material (Figure S5 in the SI), It is worth emphasizing that electrospray deposition is an appropriate method to easily form porous carbon layers on the surfaces of metal foams, maintaining good electric conduction and increasing the specific surface without the loss of total porosity. In addition, the thickness and uniformity of the carbon layers are also controllable.

**Electrochemical Properties of Carbon-Coated Metal Foam Electrodes.** The electrochemical performance of the carbon-coated metal foams was examined using CV measurements carried out over a voltage range from −2.0 to 0 V (vs $Ag/Ag^+$) for $[Co(bpy)_3]^{+/2+}$ and from −0.5 to 1.5 V for $[Fe(bpy)_3]^{2+/3+}$ at various scan rates from 5 to 200 mV $s^{-1}$. The

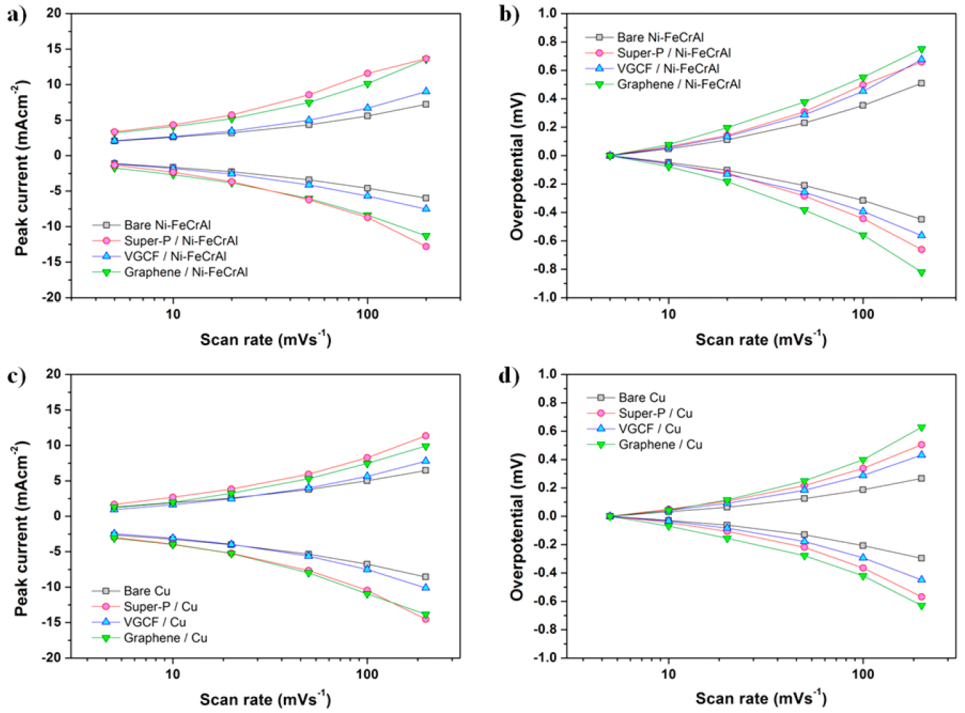


**Figure 5.** Electrochemical properties of metal foams: (a) peak currents and (b) overpotentials for Ni-FeCrAl foams after coating with various carbon materials and (c) peak currents and (d) overpotentials for Cu foams after coating with various carbon materials. The data were obtained from CV profiles recorded at different scan rates of 5, 10, 20, 50, 100, and 200 mV $s^{-1}$.

concentrations of the electrolytes were fixed at 0.2 M to control the effect of the electrolyte concentration. Parts a and b of Figure 5 show the normalized peak currents and overpotentials as a function of the applied scan rates, respectively. The peak currents for the oxidation and reduction of $[Fe(bpy)_3]^{2+/3+}$ increased after carbon deposition. In the case of the Super-P/Ni-FeCrAl foam, the peak current is about 2 times higher than that of the bare Ni-FeCrAl foam. The graphene/Ni-FeCrAl foam shows a comparable increase in the peak current, while the VGCF/Ni-FeCrAl foam exhibits a relatively small increase in the peak current. These results are consistent with the increase in the specific surface area of the metal foams induced by carbon deposition. Therefore, it is plausible that the peak current is highly dependent on the specific surface of the deposited carbon materials.

A different tendency was observed in the overpotentials, as presented in Figure 5b. The overpotentials for the redox reaction of $[Fe(bpy)_3]^{2+/3+}$ were also estimated on the basis of the redox potential obtained at a scan rate of 5 mV $s^{-1}$. In contrast with the peak currents, the graphene/Ni-FeCrAl foam exhibited the highest overpotential for the redox reactions. The Super-P/Ni-FeCrAl foam also showed an increase in the overpotential, but it is less than that shown by the graphene/Ni-FeCrAl foam. This result can be reasonably explained by the higher electrical conductivity of the Super-P layer. The electrical conductivity of the Super-P layer was measured as $9.7 \times 10^4$ S $cm^{-1}$, which was higher than that of the graphene layer ($1.4 \times 10^1$ S $cm^{-1}$). The difference might originate from the different morphologies and electrical conductivities of the deposited carbon materials.

Although the graphene layer also effectively provides more reaction sites for the redox reaction via the formation of abundant macroscopic pores, it possesses a limited electrical-pathway-forming capacity because of its two-dimensional structure, and this results in lower electrical conductivity. For this reason, the Super-P/Ni-FeCrAl foam was selected as the material for the positive electrode in a compromise between the peak current and overpotential to maximize cell performance. We conducted the same characterization of the $[Co(bpy)_3]^{+/2+}$ redox couple using carbon-coated Cu foams as well, and the results are given in Figure 5c,d. Both the graphene/Cu and Super-P/Cu foams exhibited much higher peak currents than the bare Cu foam, even more than the VGCF/Cu foam. Because of the large overpotential of the graphene/Cu foam, the Super-P/Cu foam was selected as the negative electrode in our proposed system for the same reasons as the Ni-FeCrAl foam was selected.

We examined the morphological changes in the Super-P/Ni-FeCrAl and Super-P/Cu foams after the CV measurements (1000 cycles) to verify the mechanical and chemical stabilities of the carbon-coated metal foams (Figure S6 in the SI). The uniform, porous carbon layers formed on the surfaces of the metal foams maintained their porous structure without significant degradation, even after 1000 cycles. This result reveals that our approach to forming porous carbon layers on the surfaces of metal foams is an innovative and effective technique to maximize their surface activity as well as mechanical stability.

**Cell Performance of a Nonaqueous RFB.** To examine the cell performance of the nonaqueous RFB employing $[Co(bpy)_3]^{+/2+}$ and $[Fe(bpy)_3]^{2+/3+}$ redox couples, we constructed a test cell composed of metal foam electrodes, bipolar plates, and an ion-exchange membrane. Of all of the candidate electrodes, the Super-P/Ni-FeCrAl and Super-P/Cu foams were installed as the positive and negative electrodes, respectively, in our test RFB cell. The electrodes and bipolar plates were placed on both sides of the membrane. As a result of circulation of the catholyte and anolyte, the chemical

reactions of dissolved active species in both electrolytes readily occur on the electrode surfaces, providing electric energy.

Figure 6a shows the galvanostatic charge and discharge profiles for the nonaqueous RFB that employs $[Co(bpy)_3]^{+/2+}$

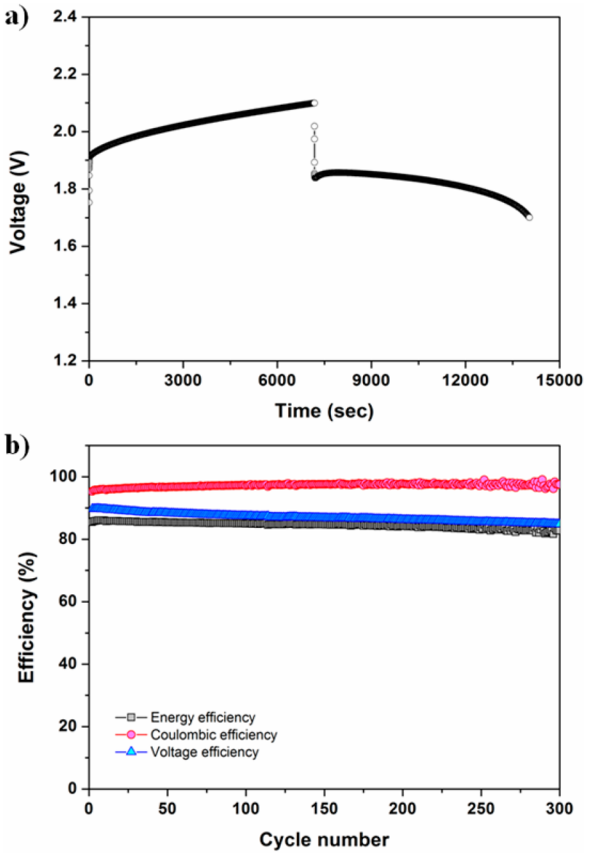


**Figure 6.** (a) Galvanostatic charge−discharge profiles for the first cycle and (b) coulombic, voltage, and energy efficiencies of the nonaqueous RFBs employing Super-P/Ni-FeCrAl (positive electrode) and Super-P/Cu (negative electrode) foams over 300 cycles.

and $[Fe(bpy)_3]^{2+/3+}$ redox couples and Super-P/Ni-FeCrAl and Super-P/Cu foams as electrodes. The cells were carefully assembled and evaluated in the voltage range between 1.7 and 2.1 V. The initial charge capacity was estimated to be 199.7 mAh, and the subsequent discharge capacity was estimated to be 190.3 mAh. Figure 6b shows the cyclic performance of the proposed nonaqueous RFB. The RFB cell exhibited initial coulombic and voltage efficiencies of 95.3 and 89.7%, respectively. The energy efficiency achieved was estimated to be 85.5%. After 300 cycles, the coulombic and voltage efficiencies were 97.5 and 84.8%, respectively. The energy efficiency was maintained up to 300 cycles with an insignificant fading of 2.8%. The use of carbon-coated metal foams as electrodes could effectively increase coulombic and voltage efficiencies by providing abundant reaction sites and minimizing contact resistance between electrodes and bipolar plates. As a result, an outstanding cyclic performance of nonaqueous RFBs could be attained. In addition, we evaluated ion crossover in the proposed system by analyzing the electrolytes with ICP-MS. After cycles, we found small traces of Co (137 ppm, equivalent to 0.0024 M) in the catholyte and Fe (260 ppm, equivalent to 0.0044 M) in the anolyte, respectively. Although the ion crossover was not serious, it should be completely prevented by adopting a suitable membrane for further improvements of the electrochemical performance and long-term stability.

To determine the mechanical and electrochemical stabilities of the Super-P/Ni-FeCrAl and Super-P/Cu foams after long-term operation, we carefully disassembled the cell and collected the metal foams after 300 cycles. To investigate the electrochemical reactivity of the Super-P/Ni-FeCrAl and Super-P/Cu electrodes after 300 cycles, we carried out CV measurements on the collected electrodes with fresh electrolytes. We confirmed that they maintained higher electrochemical reactivity, as shown in Figure 7. We could not observe

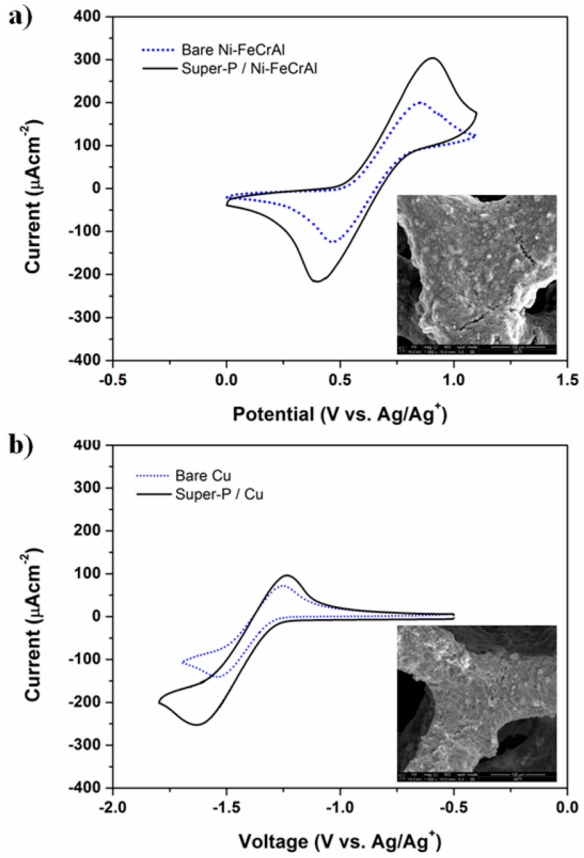


**Figure 7.** Cyclic voltammograms for (a) the Super-P/Ni-FeCrAl foam (positive electrode) and (b) the Super-P/Cu foam (negative electrode), collected after 300 cycles. FESEM images of the electrodes after 300 cycles are insets.

any change in the morphologies of both metal foams, which indicates that the carbon-coated metal foams provide sufficient mechanical stability. FESEM images of the electrodes are shown the insets in Figure 7. These results support the assertion that these carbon-coated metal foam electrodes have outstanding durability in RFBs.

## CONCLUSIONS

We proposed and constructed a nonaqueous RFB employing $[Co(bpy)_3]^{+/2+}$ and $[Fe(bpy)_3]^{2+/3+}$ redox couples and demonstrated its electrochemical properties. In an effort to improve the electrochemical performance of the nonaqueous RFB, we deposited porous carbon layers from various carbon materials. These layers can dramatically increase the specific surface area of metal foam electrodes without any loss of total

porosity and enhance redox reactions between active species in nonaqueous electrolytes. In addition, we provided a much more fundamental basis for developing nonaqueous RFBs with a wide operating voltage (>2.1 V) and high energy efficiency (>85%). Our findings are useful for developing high-energy RFBs and identifying the reaction mechanisms of new redox couples in nonaqueous systems. This study indicates a fruitful direction for further investigations on the subcomponents of nonaqueous RFBs, which could lead to a technical breakthrough in the field of energy storage.

## ■ ASSOCIATED CONTENT

### Supporting Information

Figures showing the electrospraying process, BET, and SEM images. This material is available free of charge via the Internet at http://pubs.acs.org.

## ■ AUTHOR INFORMATION


### Corresponding Authors

*E-mail: kijaekim@keti.re.kr.
*E-mail: yjkim@keti.re.kr.


### Notes

The authors declare no competing financial interest.

## ■ ACKNOWLEDGMENTS

This work was supported by the K-Initiative and the Energy Efficiency & Resources of the Korea Institute of Energy Technology Evaluation and a planning grant funded by the Korea Government Ministry of Knowledge Economy (Program 20132020000340).

## ■ REFERENCES


(1) Bartolozzi, J. Development of Redox Flow Batteries. A Historical Bibliography. *J. Power Sources* **1989**, *27*, 219−234.

(2) Leung, P.; Li, X.; de León, C. P.; Berlouis, L.; Low, C. T. J.; Walsh, F. C. Progress in Redox Flow Batteries, Remaining Challenges and Their Applications in Energy Storage. *RSC Adv.* **2012**, *2*, 10125−10156.

(3) Lee, B. S.; Gushee, D. E. Progress in Redox Flow Batteries, Remaining Challenges and Their Applications in Energy Storage. *Chem. Eng. Prog.* **2008**, *104*, S29−S32.

(4) de León, C. P.; Frías-Ferrer, A.; González-García, J.; Szánto, D. A.; Walsh, F. C. Redox Flow Cells for Energy Conversion. *J. Power Sources* **2006**, *160*, 716−732.

(5) Skyllas-Kazacos, M.; Chakrabarti, M. H.; Hajimolana, S. A.; Mjalli, F. S.; Saleem, M. Progress in Flow Battery Research and Development. *J. Electrochem. Soc.* **2011**, *158*, R55−R79.

(6) Yang, Z.; Zhang, J.; Kintner-Meyer, M. C. W.; Lu, X.; Choi, D.; Lemmon, J. P.; Liu, J. Electrochemical Energy Storage for Green Grid. *Chem. Rev.* **2011**, *111*, 3577−3613.

(7) Weber, A. Z.; Mench, M. M.; Meyers, J. P.; Ross, P. N.; Gostick, J. T.; Liu, Q. Redox Flow Batteries: A Review. *J. Appl. Electrochem.* **2011**, *41*, 1137−1164.

(8) Liu, Q.; Sleightholme, A. E. S.; Shinkle, A. A.; Li, Y.; Thompson, L. T. Non-Aqueous Vanadium Acetylacetonate Electrolyte for Redox Flow Batteries. *Electrochem. Commun.* **2009**, *11*, 2312−2315.

(9) Zhong, S.; Kazacos, M.; Burford, R. P.; Skyllas-Kazacos, M. Fabrication and Activation Studies of Conducting Plastic Composite Electrodes for Redox Cells. *J. Power Sources* **1991**, *36*, 29−43.

(10) Sun, B.; Skyllas-Kazacos, M. Chemical Modification and Electrochemical Behaviour of Graphite Fibre in Acidic Vanadium Solution. *Electrochim. Acta* **1991**, *36*, 513−517.

(11) Sun, B.; Skyllas-Kazacos, M. Modification of Graphite Electrode Materials for Vanadium Redox Flow Battery Application—I. Thermal Treatment. *Electrochim. Acta* **1992**, *37*, 1253−1260.

(12) Huang, K. L.; Li, X.; Liu, S.; Tan, N.; Chen, L. Research Progress of Vanadium Redox Flow Battery for Energy Storage in China. *Renewable Energy* **2008**, *33*, 186−192.

(13) Li, L.; Kim, S.; Wang, W.; Vijayakumar, M.; Nie, Z.; Chen, B.; Zhang, J.; Xia, G.; Hu, J.; Graff, G.; Liu, J.; Yang, Z. A Stable Vanadium Redox-Flow Battery with High Energy Density for Large-Scale Energy Storage. *Adv. Energy Mater.* **2011**, *1*, 394−400.

(14) Shinkle, A. A.; Sleightholme, A. E. S.; Thompson, L. T.; Monroe, C. W. Electrode Kinetics in Non-Aqueous Vanadium Acetylacetonate Redox Flow Batteries. *J. Appl. Electrochem.* **2011**, *41*, 1191−1199.

(15) Sleightholme, A. E. S.; Shinkle, A. A.; Liu, Q.; Li, Y.; Monroe, C. W.; Thompson, L. T. Non-Aqueous Manganese Acetylacetonate Electrolyte for Redox Flow Batteries. *J. Power Sources* **2011**, *196*, 5742−5745.

(16) Li, Z.; Li, S.; Liu, S.; Huang, K.; Wang, F.; Peng, S. Electrochemical Properties of an All-Organic Redox Flow Battery Using 2,2,6,6-Tetramethyl-1-piperidinyloxy and *N*-Methylphthalimide. *Electrochem. Solid-State Lett.* **2011**, *14*, A171−A173.

(17) Moon, J.; Lee, M. J.; Park, J. W.; Oh, D. J.; Lee, D. Y.; Doo, S. G. Non-Aqueous Redox Flow Batteries with Nickel and Iron Tris(2,2′-bipyridine) Complex Electrolyte. *Electrochem. Solid-State Lett.* **2012**, *15*, A80−A82.

(18) Leung, P. K.; de León, C. P.; Low, C. T. J.; Shah, A. A.; Walsh, F. C. Characterization of a Zinc−Cerium Flow Battery. *J. Power Sources* **2011**, *196*, 5174−5185.

(19) Leung, P. K.; León, C. P.; de Walsh, F. C. An Undivided Zinc−Cerium Redox Flow Battery Operating at Room Temperature (295 K). *Electrochem. Commun.* **2011**, *13*, 770−773.

(20) Matsuda, Y.; Tanaka, K.; Okada, M.; Takasu, Y.; Morita, M.; Matsumura-Inoue, T. A Rechargeable Redox Battery Utilizing Ruthenium Complexes with Non-Aqueous Organic Electrolyte. *J. Appl. Electrochem.* **1988**, *18*, 909−914.

(21) Liu, Q.; Sleightholme, A. E. S.; Shinkle, A. A.; Li, Y.; Thompson, L. T. Non-Aqueous Vanadium Acetylacetonate Electrolyte for Redox Flow Batteries. *Electrochem. Commun.* **2009**, *11*, 2312−2315.

(22) Yamamura, T.; Shiokawa, Y.; Yamana, H.; Moriyama, H. Electrochemical Investigation of Uranium $\beta$-Diketonates for All-Uranium Redox Flow Battery. *Electrochim. Acta* **2002**, *48*, 43−50.

(23) Wang, W.; Xu, W.; Cosimbescu, L.; Choi, D.; Li, L.; Yang, Z. Anthraquinone with Tailored Structure for a Nonaqueous Metal−Organic Redox Flow Battery. *Chem. Commun.* **2012**, *48*, 6669−6671.

(24) Kim, J. H.; Kim, K. J.; Park, M. S.; Lee, N. J.; Hwang, U.; Kim, H.; Kim, Y. J. Development of Metal-Based Electrodes for Non-Aqueous Redox Flow Batteries. *Electrochem. Commun.* **2011**, *13*, 997−1000.

(25) Sun, B.; Skyllas-Kazacos, M. Chemical Modification and Electrochemical Behaviour of Graphite Fibre in Acidic Vanadium Solution. *Electrochim. Acta* **1991**, *36*, 513−517.